References

[1] *A.A.Vorobyov, G.A.Korolev, V.A.Schegelsky, G.Ye.Solyakin, G.L.Sokolov, Yu.K.Zalite.* // Nucl. Instr. Meth., 1974. V.119. P.509.

[2] *A.A.Vorobyov, G.A.Korolev, A.V.Dobrovolsky,A.V.Khanzadeev, G.E.Petrov, E.M.Spiridenkov, Y.Terrien, J.C.Lugol, J.Saudinos, B.H.Silverman, F.Wellers.* // Nucl. Instr. Meth., 1988. V.A270. P.419.

[3] *A.V.Dobrovolsky, A.V.Khanzadeev, G.A.Korolev, E.M.Maev, V.I.Medvedev, G.L.Sokolov, N.K.Terentyev, Y.Terrien, G.N.Velichko, A.A.Vorobyov, Yu.K.Zalite.* // Nucl. Phys., 1983. V.B214. P.1.

[4] *B.H.Silverman, J.C.Lugol, J.Saudinos, Y.Terrien, F.Wellers, A.V.Dobrovolsky, A.V.Khanzadeev, G.A.Korolev, G.E.Petrov, E.M.Spiridenkov, A.A.Vorobyov.* // Nucl. Phys., 1989. V.A499. P.763.

[5] *G.D.Alkhazov, S.L.Belostotsky, A.A.Vorobyov.* // Phys. Reports, 1978. V.42C. P.89.

[6] *O.G.Grebenjuk, A.V.Khanzadeev, G.A.Korolev, S.I.Manayenkov, J.Saudinos, G.N.Velichko, A.A.Vorobyov.* // Nucl. Phys., 1989. V.A500. P.637.

[7] *G.N.Velichko, A.A.Vorobyov, O.G.Grebenyuk, G.A.Korolev, J.Saudinos, A.V.Khanzadeev.* // Yad. Fiz., 1988. V.47. P.1185.

[8] *G.N.Velichko, A.A.Vorobyov, A.V.Dobrovolsky, G.A.Korolev, S.I.Manayenkov, J.Saudinos, A.V.Khanzadeev.* // Yad. Fiz., 1985. V.42. P.1325.

[9] *G.D.Alkhazov, S.L.Belostotsky, Yu.V.Dotsenko, O.A.Domchenkov, N.P.Kuropatkin, V.N.Nikulin.* // Yad. Fiz., 1985. V.41. P.561.

[10] *S.I.Manayenkov.* // Yad. Fiz., 1993. V.56. P.126.

[11] *S.I.Manayenkov.* // Yad. Fiz., 1988. V.48. P.1260.

[12] *V.N.Gribov.* // Zh.Tekhn.Fiz., 1969. V.56. P.892.

[13] *L.G.Dakhno and N.N.Nikolaev.* // Nucl. Phys., 1985. V.A436. P.653.

[14] *J.P.Burq, M.Chemarin, M.Chevallier, A.S.Denisov, T.Ekelof, J.Fay, P.Grafstrom, L.Gustafsson, E.Hagberg, B.Ille, A.P.Kashchuk, G.A.Korolev, A.V.Kulikov, M.Lambert, J.P.Martin, S.Maury, J.L.Paumier, M.Querrou, V.A.Schegelsky, I.I.Tkach, M.Verbeken, A.A.Vorobyov.* // Nucl. Phys., 1981. V.B187. P.205.

[15] *V.G.Ableev, V.D.Apokin, A.A.Vorobyov, G.N.Velichko, Yu.K.Zalite, G.A.Korolev, E.N.Maev, Yu.A.Matulenko, S.B.Nurushev, N.M.Piskunov, V.S.Seleznev, V.V.Saksin, I.M.Sitnik, V.L.Solovyanov, E.A.Strokovsky, L.N.Strunov, N.K.Terentyev, A.V.Khanzadeev, V.I.Sharov, V.A.Schegelsky.* // Yad. Fiz., 1981. V.34. P.769.

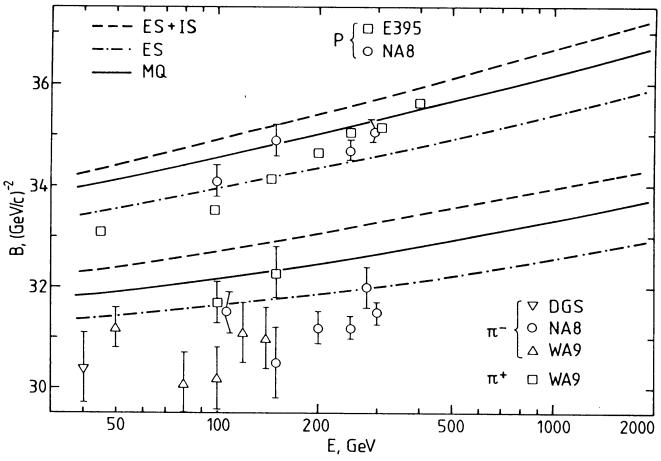

Fig. 8. Theoretical and experimental diffraction cone slopes. Legends for curves and experimental points are the same as in Fig. 7.

$$\sigma_{hB} = \pi\alpha_s^2 N_B N_h \frac{R_B^2 R_h^2}{R_B^2 - R_h^2} \ln(R_B^2/R_h^2) \; . \tag{3}$$

In (3) α_s is the QCD coupling, N_h and N_B are the numbers of quarks in a hadron and in a bag with radii R_h and R_B, respectively. If we put in (3) $N_B = 3$ and $R_B = R_N$ we obtain the total hadron-nucleon cross section. Then we can get a ratio of the cross section of nucleon scattering ($N_h = 3$, $R_h = R_N$) on the $12q$-bag to that of nucleon scattering on four nucleons, which is equal to $\sigma(N-12q)/[4\sigma(NN)] = \xi(\xi-1)^{-1}\ln(\xi)$ where $\xi = R_B^2/R_N^2$. In accordance with the MIT bag model, $R_{12q} = \sqrt{2}R_N$. So we have $\sigma(N-12q)/[4\sigma(NN)] = 2\ln 2 \approx 1.4$. The physical reason for the cross section of nucleon scattering on the $12q$-bag being larger than $4\sigma(NN)$ is as follows. The gluon exchange between the incident nucleon and a colourless system (another nucleon or the $12q$-bag) is impossible for soft gluons with a wave length λ which is larger than the radius of the system, because the soft gluons interact not with separate quarks but with the total colour charge of the colourless system, which is equal to zero. For the nucleon-nucleon interaction $\lambda \leq R_N$, meanwhile for the nucleon interaction with the $12q$-bag $\lambda \leq R_B = \sqrt{2}R_N$. We see that in the latter case softer gluons do contribute to the interaction, and the total cross section is larger than in the former case.

Let us summarize the main points of the discussion of $p\alpha$ and $\pi\alpha$ elastic scattering. There is an appreciable discrepancy between the differential cross sections of p^4He scattering at intermediate energies calculated in the framework of the Glauber theory and the high precision experimental data at small scattering angles ($|t| \leq 0.08$ (GeV/c)^2). The discrepancy cannot be explained by known corrections to the diffraction multiple scattering theory by Glauber and Sitenko. It is not excluded, in principal, that the applied nuclear wave functions were not realistic enough to describe the data well. But, perhaps, correct description of the α-particle structure and its interaction with hadrons needs to go beyond the common physical picture of the ^{4}He nucleus as a system of four nucleons. The discrepancy between the calculations and the experimental data on the total and differential cross sections of p^4He and π^4He scattering at high energies has been removed with the hypothesis assuming an admixture of the $12q$-bag to the ground state of the ^{4}He nucleus. But this interesting hypothesis should be checked in other phenomena. In the ideal case, the quark wave function of ^{4}He should be obtained in some dynamical quark model, but this outstanding problem is very far from its solution for the time being.

account. In Ref. [13], a phenomenological wave function of ^{4}He (a product of single particle wave functions) has been applied. The nucleon-nucleon correlations due to the short-range repulsion in the NN potential are shown to be unessential for the studied processes. Dakhno and Nikolaev have succeeded to describe well the charge form factor of the α-particle up to $q^2 = 0.8$ (GeV/c)^2 in the two best fits in Ref. [13], both the proton and neutron charge form factors being taken into account. Theoretical uncertainties of the IS contributions to the total $p\alpha$ cross section are less than 0.6 mb [13]. Fig. 7 shows that the experimental total p^4He cross sections [14], having the error of the absolute normalization less than 1%, lie systematically above the calculated ones by 2–3 mb. In case of $\pi\alpha$ diffraction scattering, the experimental total cross sections are systematically above the theoretical ones by 1–2 mb too. Having taken into account the inelastic shadowing effects, the calculated slope parameter b for $p\alpha$ scattering exceeds its experimental value by ~ 1 (GeV/c)$^{-2}$ as one can see from Fig. 8. For $\pi\alpha$ elastic scattering the discrepancy between the calculated and experimental diffraction cone slope is about 2 (GeV/c)$^{-2}$.

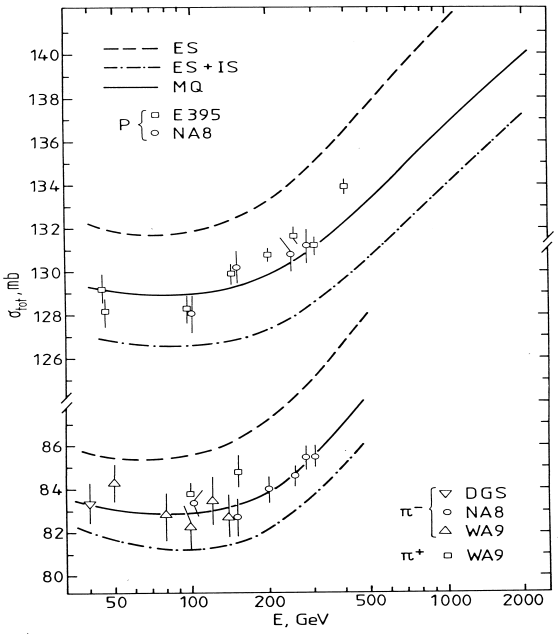

Fig. 7. Calculated and experimental $p\alpha$ and $\pi\alpha$ total cross section. WA9, NA8 points are taken from Ref. [14], DGS data are those of Ref. [15], E395 data are obtained by Nikitin et al. (1981). Curve legends: for ES curve only elastic shadowing was included; ES+IS means elastic and inelastic shadowing; for MQ curve contribution of $12q$-bag is added.

To achieve an agreement of the calculations with the experimental data, Dakhno and Nikolaev supposed that there is a 12% admixture of the 12-quark bag in the ground state of ^{4}He. In the MIT bag model, the $12q$-bag radius is equal to $\sqrt{2}r_p = 1.15$ fm. It is smaller than the radius of the nucleon component of ^{4}He ($r_{He} \approx 1.5$ fm). The amplitudes of elastic π-$12q$ and p-$12q$ scattering decrease slower with an increase of $|t|$ than the usual Glauber amplitude. The $12q$-bag admixture reduces b and improves agreement with the experimental data (see Fig. 8). It moves the calculated diffraction minimum position to a higher value of $|t|$, which agrees with the experimental data. To understand the reason of the total cross section increase let us consider the formula for the total cross section of hadron scattering on a bag B:

like to stress that the pd cross sections are most sensitive to the same NN amplitudes as the $p\alpha$ cross sections [6] (namely, to the scalar and spin-orbital amplitudes). Another explanation supposes that the radius of the neutron density in ^{4}He is smaller than the radius of the proton density by $\Delta r \approx 0.2$ fm [9]. This hypothesis assumes, however, a serious violation of the isotopic invariance of the strong interaction because such difference between the radii of the neutron and proton densities in ^{4}He cannot be explained by the Coulomb repulsion of the protons.

The Fresnel corrections to the amplitudes in the Glauber approximation, the Fermi motion of nucleons in ^{4}He, the charge exchange and excitation of the $\Delta(1232)$ isobar in intermediate states have been taken into account in Ref. [6]. Every effect mentioned above gives corrections comparable with statistical errors of the data [6,8], hence it has to be considered. But none of them can be responsible for the 20% discrepancy in the $p\alpha$ cross section at $-t = 0.08$ (GeV/c)^2 shown in Fig. 6. The wave function of ^{4}He in Ref. [6] was a phenomenological one. Its two free parameters have been determined by fitting the world's data on the e^4He scattering at $|t| \leq 0.4$ (GeV/c)^2. The wave function used in Ref. [6] had no D-wave component. However, the calculations [10] with two realistic wave functions of ^{4}He (they were the solutions of the Schrödinger equation with realistic NN potentials) have shown that the D-wave contribution cannot solve the problem.

It is now generally accepted that the nucleon consists of quarks interacting through the gluon exchange. The quark wave function obeys the Pauli principle. Hence the electric charge density is changed when nucleons are close to each other (when the distance is comparable with the nucleon radius). This effect causes a violation of relation (2). The Helium radius r_{He} due to the quark exchange integral contributions (the number of them is equal to 15399) can be smaller than that given by (2). The Pauli blocking effect could give a key for understanding the difference between the calculated and experimental diffraction cone slopes of $p\alpha$ scattering. But, as it was shown in Ref. [11], the expectations of appreciable quark statistics effects which are based on small distances between nucleons in the α-particle ($r_{ch} = 1.67$ fm, $r_p = 0.8$ fm), turn out to be in vain. The correction to r_{He} is $\sim 10^{-2}$ fm [11], which is about ten times smaller than the needed value. The reason of the smallness of the quark statistics effects is the following. The exchange integrals are proportional to λ^n ($n = 1, 2, 3, 4$) with n corresponding to the number of the overlapping quark wave functions of nucleons, and λ is small. Indeed, λ is equal to $(r_p/r_{He})^3/N_q$ where $(r_p/r_{He})^3 \approx 0.1$ is the space factor and $N_q = 12$ denotes the number of internal degrees of freedom of a quark (spin, isospin, and colour). Besides, contributions of different quark permutations cancel each other considerably, so the net effect is very small.

Thus, the problem of description of the slope parameter of the differential cross section of $p\alpha$ elastic scattering in the framework of the common nuclear physics is not solved. This fact shows probably that non-nucleonic degrees of freedom are to be taken into consideration.

$p\alpha$ and $\pi\alpha$ elastic scattering at high energies

At high energies, the incident hadron interacting inelastically with a nucleon in the nucleus can be transferred into an excited state (a resonance or a shower of particles). After some number of rescatterings, the excited state can come back to the initial state. The Glauber theory has to be corrected at high energies to take into account the process discussed above, which is called the inelastic shadowing (IS) [12]. Dakhno and Nikolaev [13] have calculated the cross sections of the elastic p^4He and π^4He scattering at high energies and compared them with the data obtained by Vorobyov et al. [14,15] and by Nikitin et al. (1981), the inelastic shadowing being taken into

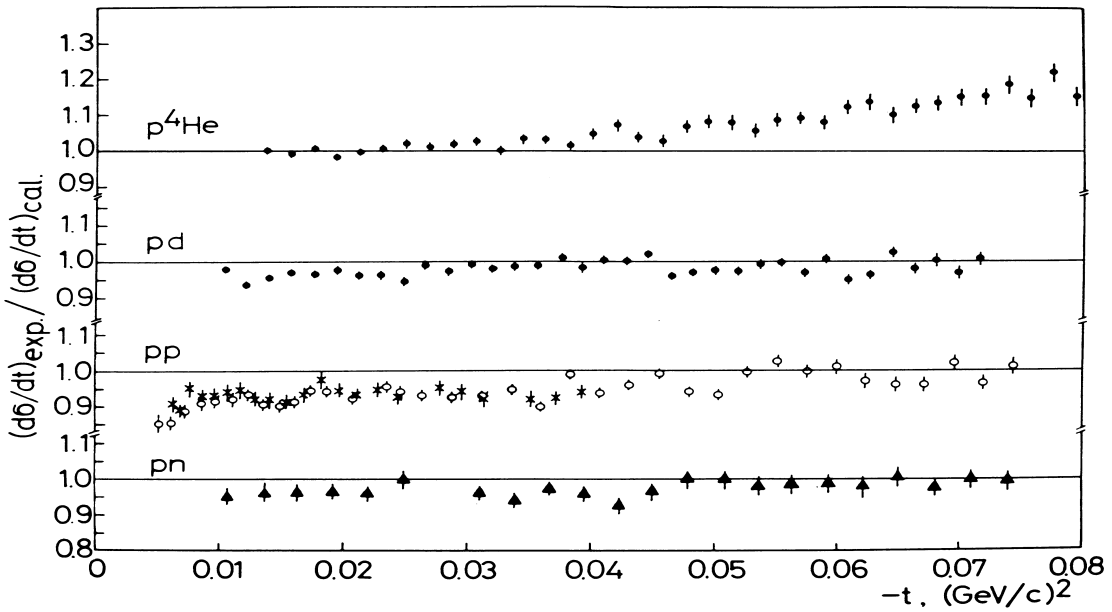

Fig. 6. Ratio of experimental cross sections to calculated ones at T_0 = 992 MeV. Experimental data on pd and p^4He scattering are taken from Refs. [6,7], and pp, np data are obtained in Refs. [3,4], respectively. Details of calculations see in Refs. [6,8].

all measurements performed at the energies 695, 793, 890, and 991 MeV [6,8]. It corresponds to the difference of 2–3 $(\mathrm{GeV/c})^{-2}$ between the calculated slope parameter b of the differential cross section of p^4He scattering and the experimental one. Though this difference is less than 10% of the value of b for p^4He scattering (b = 28 $(\mathrm{GeV/c})^{-2}$ [6]), the difference is essential as it is comparable with b_{pp} and b_{np} at T_0 = 1 GeV (see Fig. 4a). It is interesting to understand the difference between the calculations presented in Fig. 6 and the previous ones done by Bassel and Wilkin who described well the experimental data. First, the contribution of the neutron charge form factor was ignored in the previous works. Taking into account the neutron charge radius r_n, we increase the radius of ^{4}He according to the relation

$$r_{He}^2 = r_{ch}^2 - r_p^2 - r_n^2 \,, \tag{2}$$

as the "square" of the neutron charge radius is negative and equal to –0.126 fm^2 (Yu.A.Alexandrov et al., 1986). In (2) r_{ch} is the charge radius of ^{4}He. Borie and Rinker (1978) found it to be equal to 1.673 $\pm$ 0.001 fm. In Ref. [6] the proton charge radius was put equal to 0.812 fm. The contribution of the neutron charge form factor in (2) increases the calculated value of b by about 1 $(\mathrm{GeV/c})^{-2}$. This statement was first done in Ref. [9]. Second, Bassel and Wilkin took into account the scalar pp and np amplitudes only, their slope parameters being put equal to the corresponding value for the differential cross section of pp elastic scattering. In Ref. [6] all the invariant NN amplitudes under consideration have been taken from the phase shift analysis by Arndt (1987). Contributions of the spin-spin NN amplitudes to p^4He scattering at small $|t|$ are negligible [6]. The scalar and spin-orbital NN amplitudes give the main contributions to the cross section of p^4He scattering. It is very important that the slope parameters of the scalar amplitudes are by 1.5–3 $(\mathrm{GeV/c})^{-2}$ larger than those for the differential cross sections. We might suppose that PSA overestimates the values of b_{pp} and b_{np} but this hypothesis contradicts to the good description of the pd scattering data (see Fig. 6) with the same NN amplitudes. We would

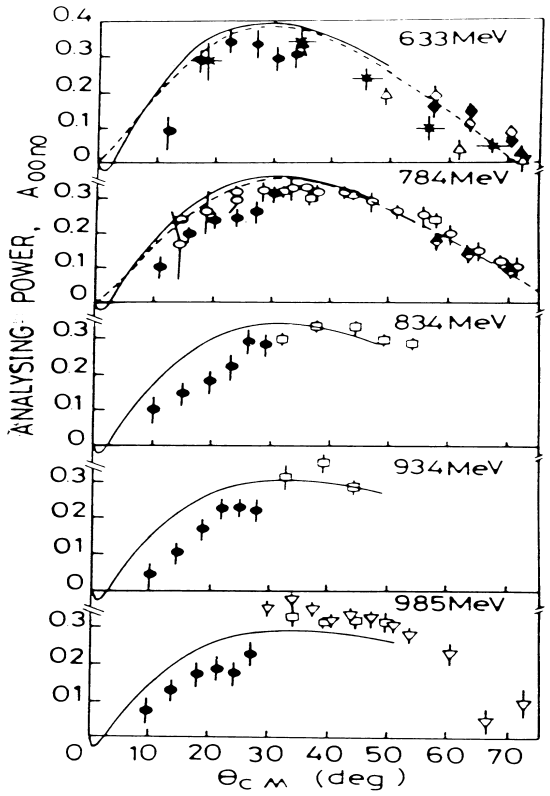

Fig. 5. Analyzing power of *np* elastic scattering. Curves show results of phase shift analyses by Arndt et al. and Lehar et al. Solid points represent experimental data of Ref. [4] where one can find all the references.

Elastic scattering of protons from the lightest nuclei at intermediate energies

Hadron-nucleus scattering at small angles for energies ≥ 1 GeV is usually described by the diffraction multiple scattering theory proposed by Glauber and Sitenko. It has been applied successfully for description of pion and proton scattering on many nuclei, from the deuteron to the lead [5]. The calculations performed by Bassel and Wilkin in the framework of the Glauber theory have demonstrated a reasonable agreement with the pioneering Brookhaven data on elastic scattering of 1 GeV protons on ^{2}H, ^{4}He, ^{12}C, and ^{16}O. The simple oscillator wave functions for ^{12}C and ^{16}O were used. Description of the proton scattering on ^{2}H and ^{4}He needed more complicated nuclear models. Omitting details of the dramatic history of the *pd* scattering investigation, we can presumably constate that, after taking into account both the *D*-wave component of the wave function and all the five *NN* amplitudes, the problem of description of the *pd* scattering was solved. Comparison of the cross sections measured using the recoil detector IKAR at $T_0 = 992$ MeV [3,4,6–8] with the theoretical predictions is presented in Fig. 6. One can see that the calculations are in excellent agreement with the high precision data for the deuteron (statistical accuracy about 1–3% and the error of the absolute normalization $\leq 2\%$). On the other hand, one can see from Fig. 6 that for ^{4}He the ratio of the experimental cross section to the theoretical one grows with the increase of $|t|$. This discrepancy exists for

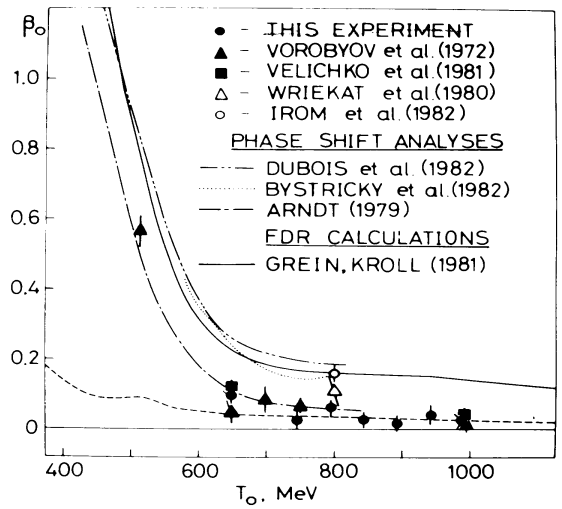

Fig. 3a. Energy dependence of β_0 for pp scattering. Solid line represents forward dispersion relation (FDR) calculations. Other curves show phase shift analyses results. This figure has been taken from Ref. [3].

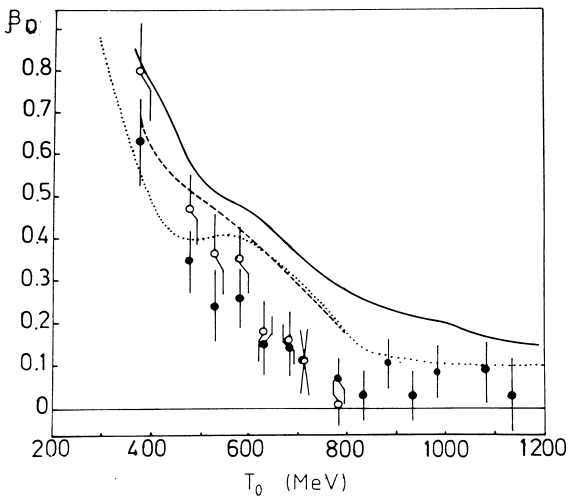

Fig. 3b. Energy dependence of β_0 for np scattering. Dotted curve represents FDR calculations. Other curves show phase shift analyses results. Solid points present experimental data of Ref. [4] from which the figure has been taken.

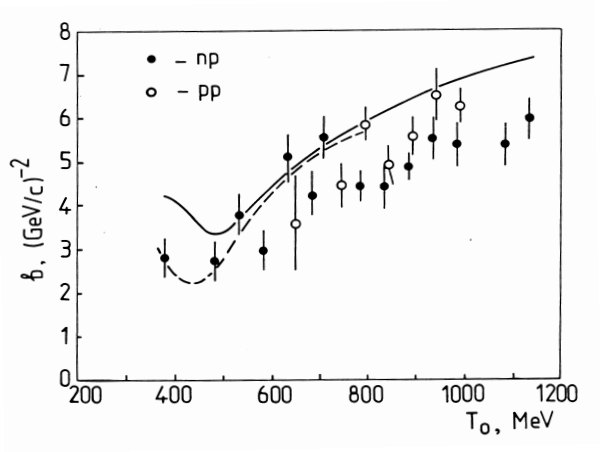

Fig. 4a. Dependence of b_{pp} and b_{np} on beam energy. Curves show phase shift analysis results. Experimental data are taken from Refs. [3,4].

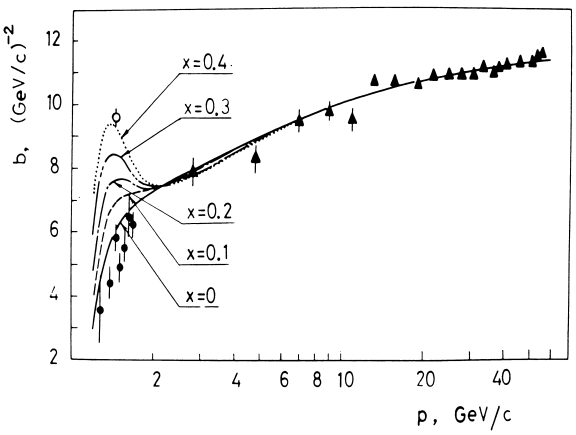

Fig. 4b. Dependence of b_{pp} on beam momentum and elasticity x of dibaryon resonance ${}^3F_3$. Triangles represent data of Beznogikh et al. (1973) and solid points are taken from Ref. [3]. Details can be found in Ref. [3].

Arndt et al. (1979, 1987) and Bystritsky et al. (1982, 1987) performed before the experimental data [3,4] have been obtained. Fig. 4b illustrates possible contributions of the ${}^3F_3$ dibaryon resonance into b_{pp}, where x denotes a probability of its decay into two protons (elasticity). We can see from Fig. 4b that the best agreement between the calculations and the experimental data is achieved at $x = 0$. There has not been found any evidence of the dibaryon resonances in the np system too. Fig. 5 shows that the phase shift analyses are in a reasonable agreement with the data [4] on the analyzing power A_{00n0}, which fill a gap in the world's data on small angle np scattering.

of a magnet with a large aperture and a set of multiwire proportional chambers (PC3–PC7). The incident beam momentum has been measured by another magnetic spectrometer. The angle between the recoil tracks and the anode plane has been determined by the rise time of the anode signal and by the difference between the appearance time of pulses on anodes A and B.

Study of nucleon-nucleon amplitudes

The nucleon-nucleon (NN) amplitudes are the input parameters for description of the diffraction scattering of hadrons on nuclei at intermediate and high energies. The experimental NN data are accumulated in phase shifts. To perform an unambiguous phase shift analysis (PSA), one has to carry out the so-called complete experiment. It consists of measurements of the differential cross sections and polarization parameters of pp and np elastic scattering at the same energy. The NN amplitudes were intensively studied in the 70s and 80s at many accelerators including the PNPI synchrocyclotron. Further on we shall restrict our discussion by the small angle scattering experiments in which the IKAR recoil detector has been used. The differential cross sections of pp elastic scattering at 650–1000 MeV with a high precision absolute normalization have been measured at Gatchina [3]. The cross sections and the analyzing powers in $\vec{n}p$ scattering have been obtained using the polarized neutron beam at Saclay in the energy range 78–1135 MeV [4].

In these experiments, the slope parameters of the differential cross sections (b) and the ratio of the sum of squares of the spin-spin amplitudes to the square of the imaginary part of the scalar amplitude (β_0) at $t = 0$ have been evaluated both for pp and for np scattering. Let us explain the main points of the method applied for np scattering. The differential cross section at small momentum transfers can be written as

$$\frac{d\sigma}{dt} = \frac{\sigma_{tot}^2}{16\pi}(1 + \rho_0^2 + \beta_0)\exp\{bt\} = \frac{d\sigma}{dt}\Big|_{t=0}\exp\{bt\}\ . \qquad (1)$$

The magnitude of the total cross section σ_{tot} for scattering of unpolarized neutrons was taken from the world experimental data. For the ratio (ρ_0) of the real to imaginary part of the scalar np amplitude at $t = 0$ we used the values calculated by Grein and Kroll (1982) using the forward dispersion relations (FDR). The free parameters β_0 and b were obtained from fitting our differential cross section data. Note that in this way the sum of squares of the np spin-spin amplitudes at $t = 0$ is determined without performing PSA. For pp elastic scattering, instead of (1) we have to use a more complicated formula to take into account the Coulomb scattering. The interference between the Coulomb and strong interactions permits to find the value of ρ_0 from the experimental differential cross section directly. This value was found to agree well with the FDR prediction. Fig. 3 shows that the value of β_0 decreases rapidly with an increase of the beam energy T_0. It becomes smaller than 0.1 already at $T_0 = 700$ MeV both for np and pp scattering. Comparison of the PSA curves with the experimental data on β_0 shows that, as a rule, the phase shift analyses overestimate the spin-spin NN amplitudes (more exactly, their real parts which are larger than the imaginary parts). This discrepancy is due to a lack of data at small angles when the phase shift analyses were performed.

The knowledge of the NN diffraction cone slope b is important for description of the nucleon-nucleus scattering. Besides, its momentum dependence can be used also for a search for the dibaryon resonances, a vital question up to now. We can see from Fig. 4a that the values of b obtained in [3,4] are in a qualitative agreement with the predictions of PSA by

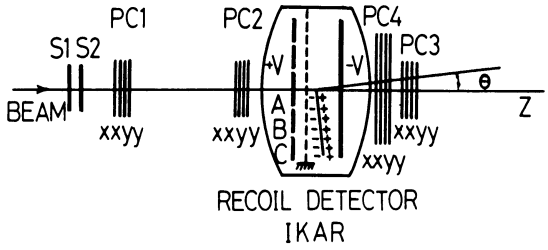

Fig. 1. Experimental setup in medium energy experiments. S1 and S2 are scintillation counters, PC1–PC4 are proportional chambers, IKAR is the detector of recoil nuclei.

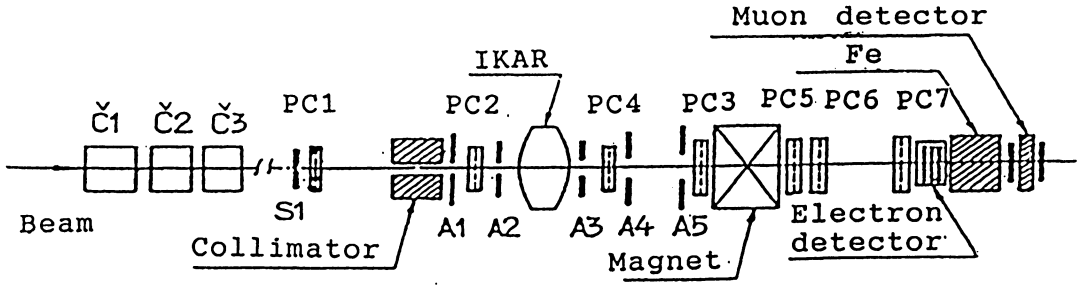

Fig. 2. Layout of experimental setup at CERN SPS. Č1 is differential Cherenkov counter, Č2, Č3 are threshold Cherenkov counters, S and A are scintillation counters and PC1–PC7 are proportional chambers.

In the setup used at intermediate energies (see Fig. 1) the proportional chambers PC1 and PC2 determined the incident particle angle. The hadron scattering angle was determined by measuring the track coordinates in the proportional chambers PC3, PC4, while the hadron-nucleus interaction point was determined with the IKAR spectrometer. The scintillation counters S1 and S2 have been used as a beam monitor. The proportional chambers PC1–PC4 and the counters S1, S2 composed a trigger system for the IKAR recoil detector. Events with the hadron scattering angle larger than some preset value have been selected. The selection coefficient was about 100. Trajectories of the scattered hadrons were near the symmetry axis of IKAR (Z-axis). Measurement of the time difference between the anode and cathode signals permits to determine Z-coordinate of the interaction point. For the elastic small angle scattering, the track of the recoil nucleus is nearly parallel to the anode A, B planes (see Fig. 1). The anodes A and B are concentric rings. If the range of the recoil nucleus is shorter than the outer radius of the anode B, the sum of the anode pulses $V_A + V_B$ is proportional to the recoil energy T_R. The recoil energy scale calibration has been done using the relation between T_R and the proton scattering angle θ at the known beam energy (1 GeV). The recoil energy resolution (σ) was about 50 keV. If the recoil nucleus goes out of the anode B zone, it looses in the sensitive volume only part of its energy; besides, $V_A + V_B$ decreases with the increase of T_R. This means that the same value of $V_A + V_B$ may correspond to two recoil energies, T_1 and T_2. The larger energy T_2 corresponds to a larger angle θ, hence by measuring θ we can find in unambiguous way the value of T_R using the calibration curve $V_A + V_B = f(T_R)$.

The layout of the experimental setup for the high energy experiments is presented in Fig. 2. For identification of the beam particles, two threshold and one differential Cherenkov counters, and also a muon detector and an electron detector have been used. The momentum of the scattered particle was measured (precision of $\Delta p/p = \pm 0.5\%$) with the spectrometer consisting

ELASTIC DIFFRACTION SCATTERING OF HADRONS ON THE LIGHTEST NUCLEI

G.N.Velichko, A.A.Vorobyov, G.A.Korolev, S.I.Manayenkov, A.V.Khanzadeev

Introduction

The experimental method elaborated at PNPI enables high precision studies of the elastic small angle scattering of pions and nucleons on hydrogen, deuterium, and helium nuclei. The main part of the experimental setup is the IKAR recoil detector which has been used for measurements both at intermediate energies (Gatchina and Saclay) and at high energies (Serpukhov and CERN). The advantage of the applied method is a possibility to measure differential cross sections with the absolute accuracy of 1–2%. The differential cross sections of elastic scattering and the analyzing powers have been measured. The total cross sections and the ratios of the real to the imaginary parts for the scalar amplitudes of studied processes have been found. Experimental upper bounds for nucleon-nucleon (NN) spin-spin amplitudes have been derived. The experimental data under discussion help to determine phase shifts of NN scattering and in many cases clarifies the problem of dibaryon resonances which are a matter of current interest up to now. The obtained experimental hadron-nucleus total cross sections permit to study the inelastic shadowing corrections to the cross sections calculated in the framework of the Glauber theory. Also, the high precision PNPI data propounded some new problems not solved up to now. In this review, we discuss shortly the experimental method and the obtained experimental results emphasizing the unsolved physical problems related to these results.

Experimental setup

The experimental setup was not much different for different experiments, so we shall describe here its main features only. A detailed description of the experimental apparatus shown in Figs. 1,2 can be found in Refs. [1,2]. The ionization chamber (IKAR) filled with pure gas (^{1}H, ^{2}D, ^{4}He, CH_4) at 10–15 atm pressure was a target and a detector of recoils (p, d, ^{4}He) simultaneously. Besides, the hadron scattering angle θ has been measured with a system of multiwire proportional chambers which eliminated significantly the background events. The four-momentum transfer squared was determined as $-t = 2M_R T_R$ where M_R and T_R denote the mass and the kinetic energy of the recoil nucleus (detected by IKAR), respectively. The resolution $\Delta t \sim 10^{-4}$ (GeV/c)^2 can be achieved in this case. This method is most effective at small t, especially in the region of interference of the Coulomb and strong interaction amplitudes. Another method for determination of the t values used the relation $|t| = p^2\theta^2$, where p denotes the incident particle momentum. The latter method has been applied at larger (~ 200 MeV/c) momentum transfers.